Paper Presentation

Vivek Yadav
(CY20D751)

nature communications

Article

https://doi.org/10.1038/s41467-024-54030-6

Photosynthesis of Au_8Cu_6 nanocluster for photocatalysis in oxidative functionalization of alkynes

Received: 11 March 2024

Accepted: 28 October 2024

Published online: 07 November 2024

Yan Zhao[1,3], Ze-Min Zhu[1,3], Weigang Fan[1,3], Wanli Zhu[1], Jing-Jing Yang[1], Yang Tao[2], Wenwen Fei[1], Hong Bi[2], Sheng Zhang[1] ✉ & Man-Bo Li[1] ✉

- [1]Key Laboratory of Structure and Functional Regulation of Hybrid Materials of Ministry of Education, Institutes of Physical Science and Information Technology, Anhui University, Hefei, P. R. China.
- [2]School of Materials Science and Engineering, Anhui University, Hefei, P. R. China.

NANO LETTERS

pubs.acs.org/NanoLett

Letter

Photochemical Route for Synthesizing Atomically Precise Metal Nanoclusters from Disulfide

Ze-Min Zhu,[§] Yan Zhao,[§] Hongliang Zhao, Chang Liu, Ying Zhang, Wenwen Fei, Hong Bi, and Man-Bo Li*

Cite This: *Nano Lett.* 2023, 23, 7508−7515

Read Online

ACCESS | Metrics & More | Article Recommendations | Supporting Information

ABSTRACT: Practical approaches to the synthesis of atomically precise metal nanoclusters are in high demand as they provide the structural basis for investigating nanomaterials' structure−property correlations with atomic precision. The Brust−Schiffrin method has been widely used, while the essential reductive ligands (e.g., thiols) limit the application of this method for synthesizing metal nanoclusters with specific frameworks and surface ligands. In this work, we developed a photochemical route for synthesizing atomically precise metal nanoclusters by applying disulfide, which is a widely available, stable, and environmentally friendly sulfur source. This method enables the construction of structurally diverse metal nanoclusters and especially features the synthesis of PhS-protected metal nanoclusters that were not easily achieved previously and the gram-scale synthesis. A reduction−oxidation cascade mechanism has been revealed for the photochemical route. This work is expected to open up new opportunities for metal nanocluster synthesis and will contribute to the practical applications of this kind of nanomaterial.

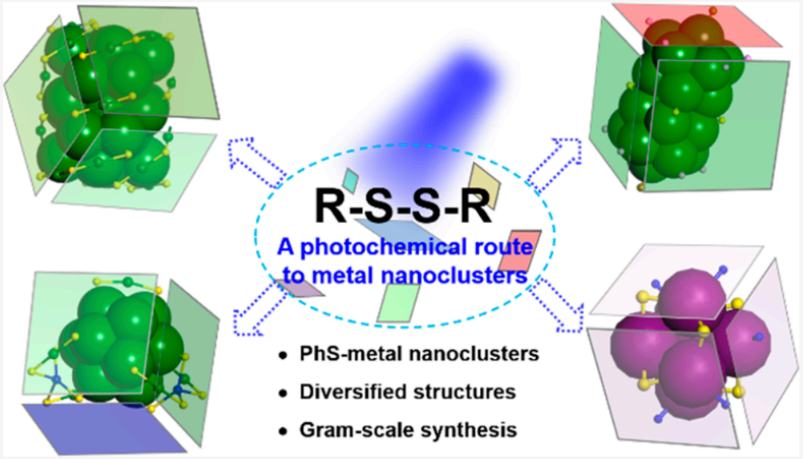

KEYWORDS: *photochemical route, metal nanocluster, disulfide, reduction−oxidation cascade mechanism, gram-scale synthesis*

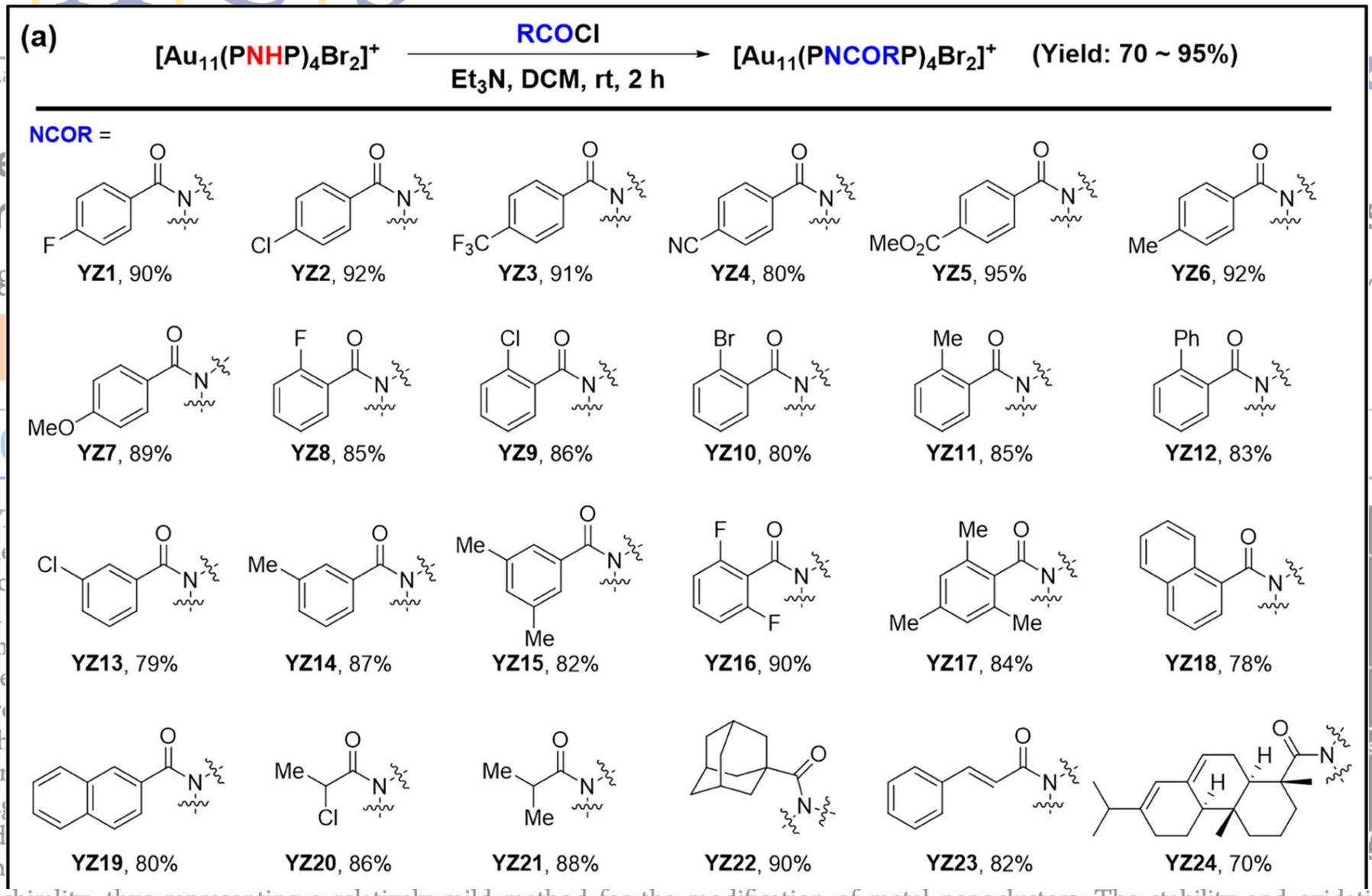

and chirality, thus representing a relatively mild method for the modification of metal nanoclusters. The stability and oxidation barrier of the Au_{11} nanocluster are also improved accordingly. The method developed here would be a generalizable strategy for the precision functionalization of metal nanoclusters.

Introduction

Why this paper?

- This group focuses on the construction of functional metal nanoclusters for catalyzing organic transformations.
- Very recently, they developed a photochemical route for synthesizing atomically precise metal nanoclusters from disulfide. A reduction–oxidation cascade mechanism was revealed for this synthetic route, which is quite different from the conventional reduction synthesis of metal nanoclusters.

Overall idea of this paper.

- Benefiting from the photochemical process, the as-synthesized nanoclusters feature high structural stability toward light irradiation and oxidation conditions. Inspired by the achievements, they envisioned the possibility of synthesizing new metal nanoclusters by the photochemical route and applying them in photocatalysis.
- In this work, they have synthesized an Au-Cu alloy nanocluster, which features a stable structure with formally full +1 charged gold and copper atoms on the surface.
- The abundant activation sites along with the high stability endow this nanocluster with catalytic performance in the functionalization of alkynes under oxidative conditions.

1

(a) Photosynthesis

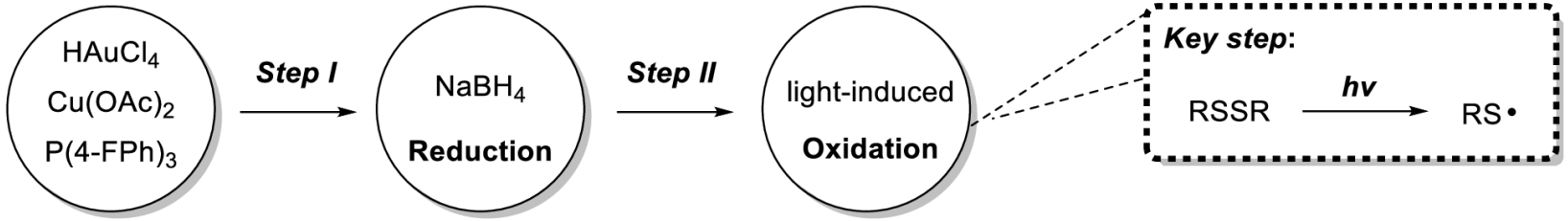

(b) Precise structure

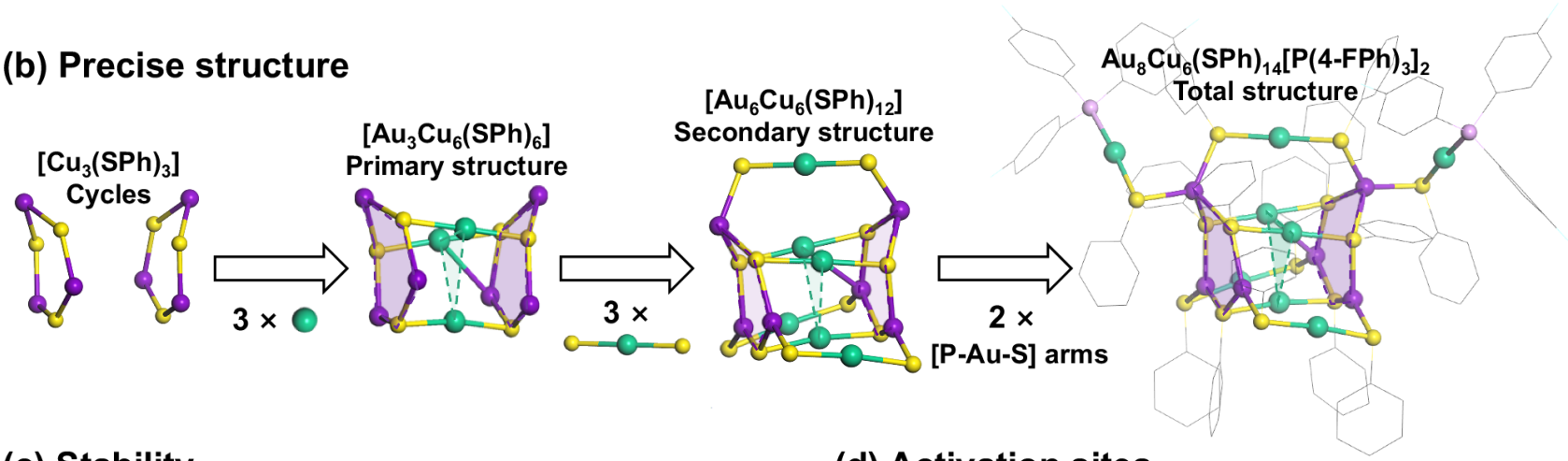

(c) Stability

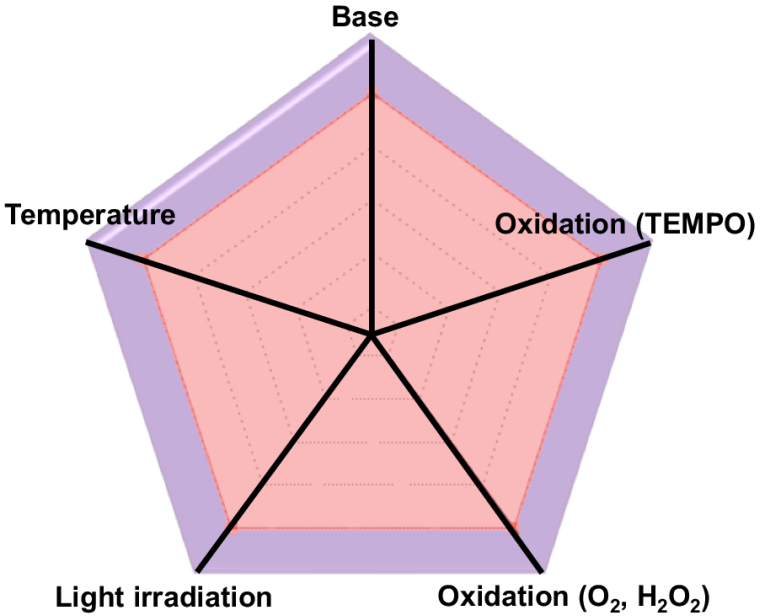

(d) Activation sites

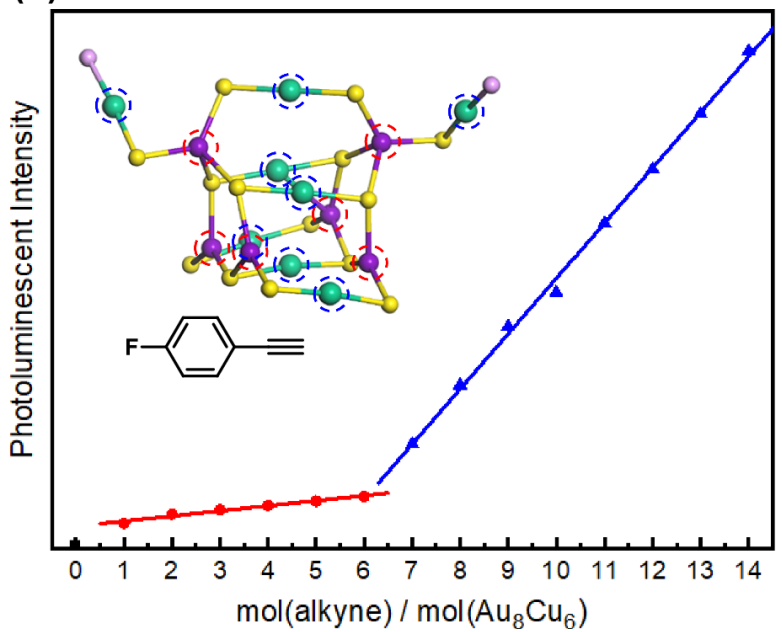

1

(a) Photosynthesis

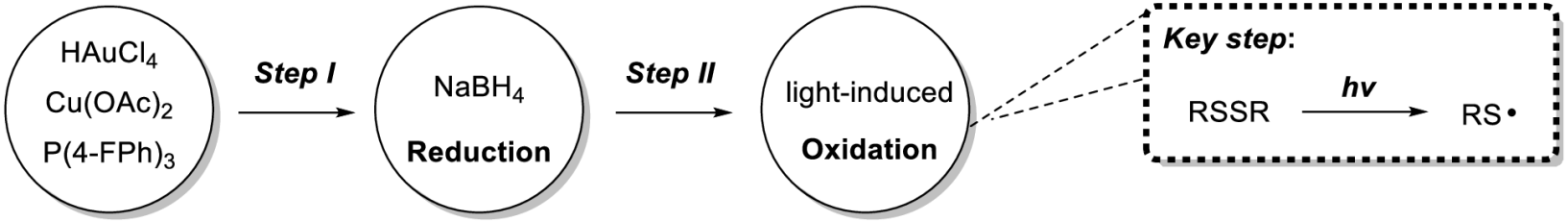

(b) Precise structure

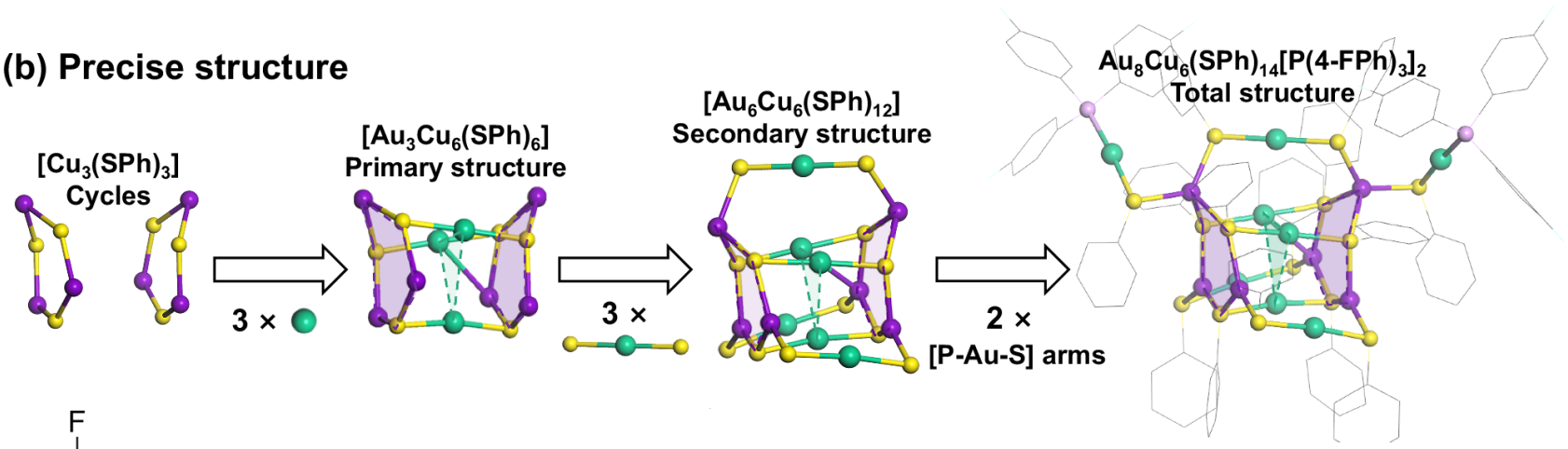

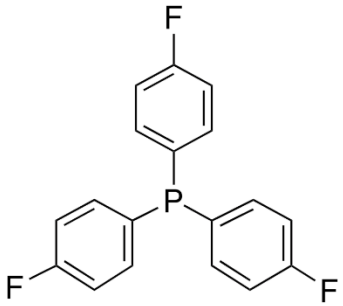

P(4-FPh)

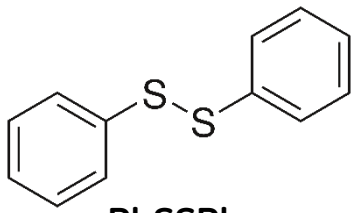

PhSSPh

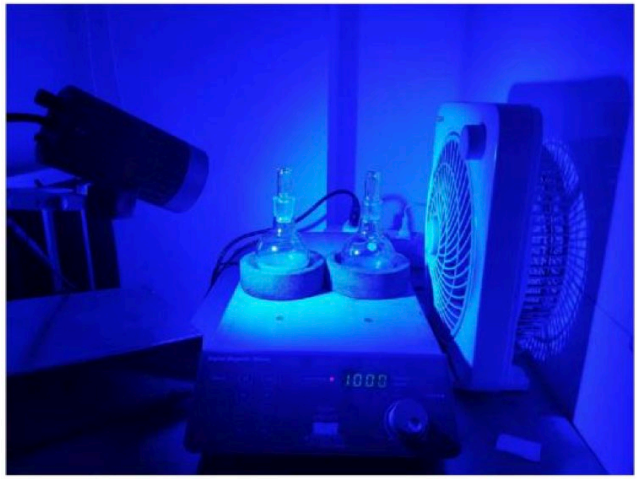

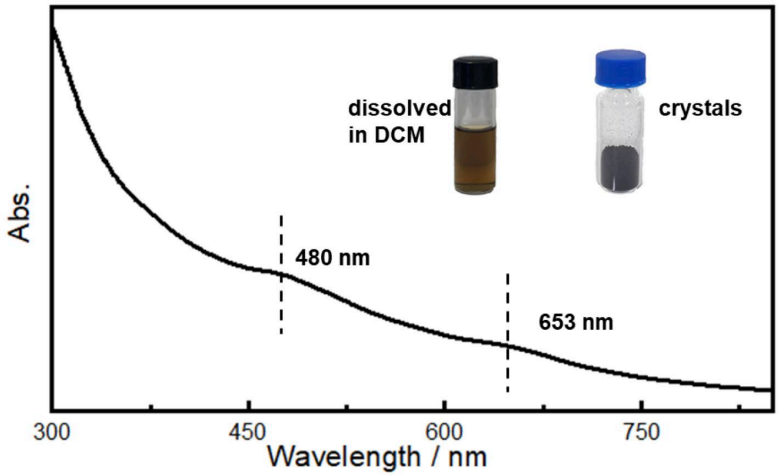

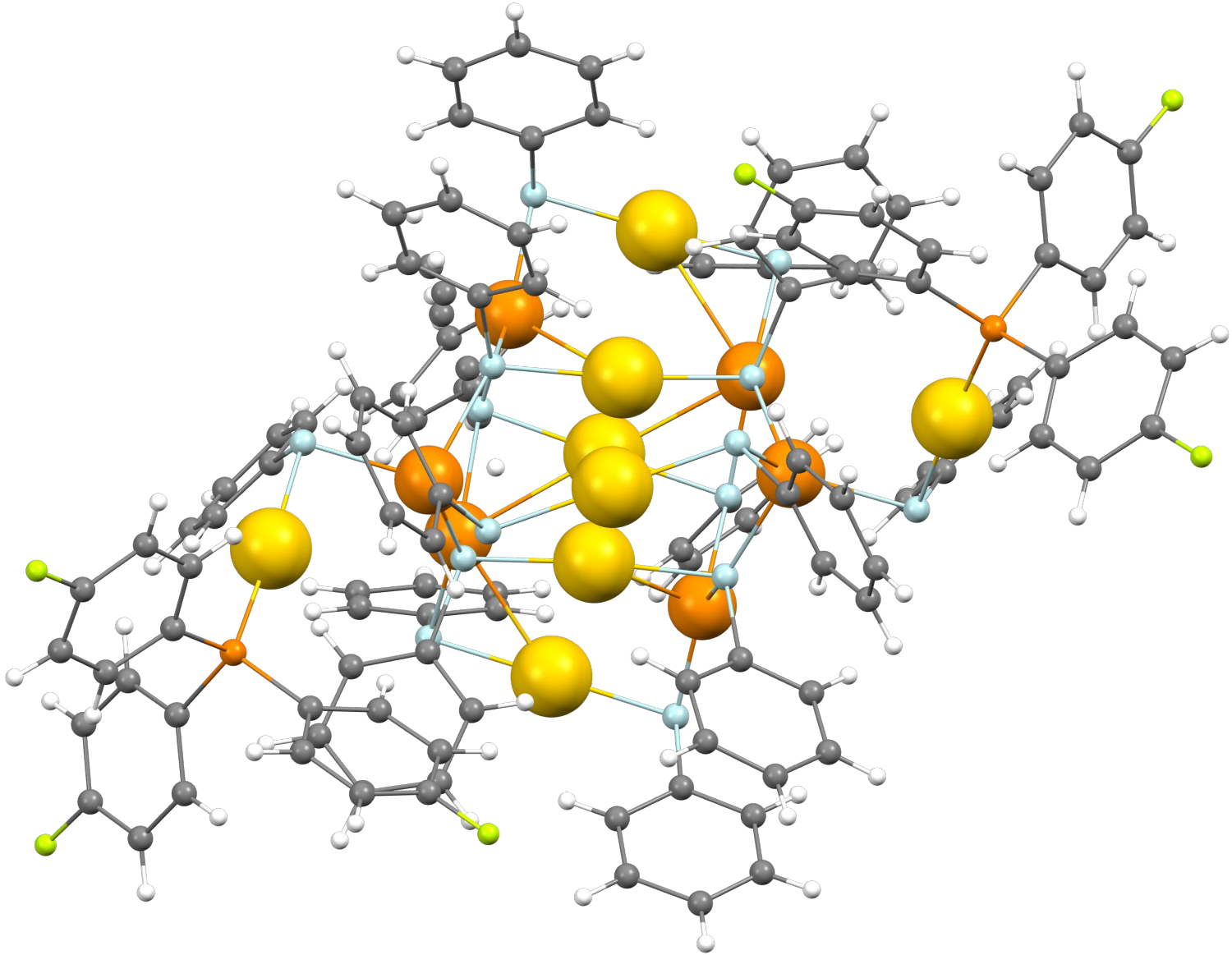

$Au_8Cu_6(SPh)_{14}[P(4\text{-}FPh)_3]_2$

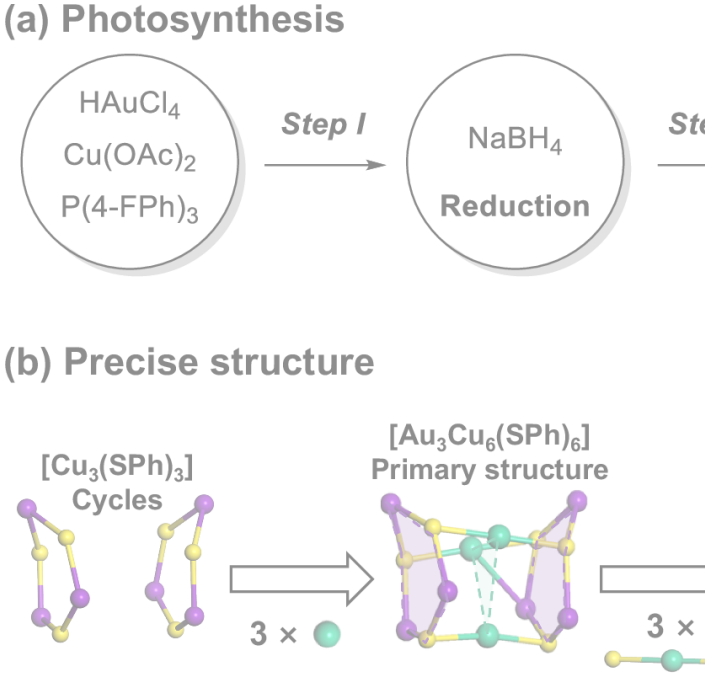

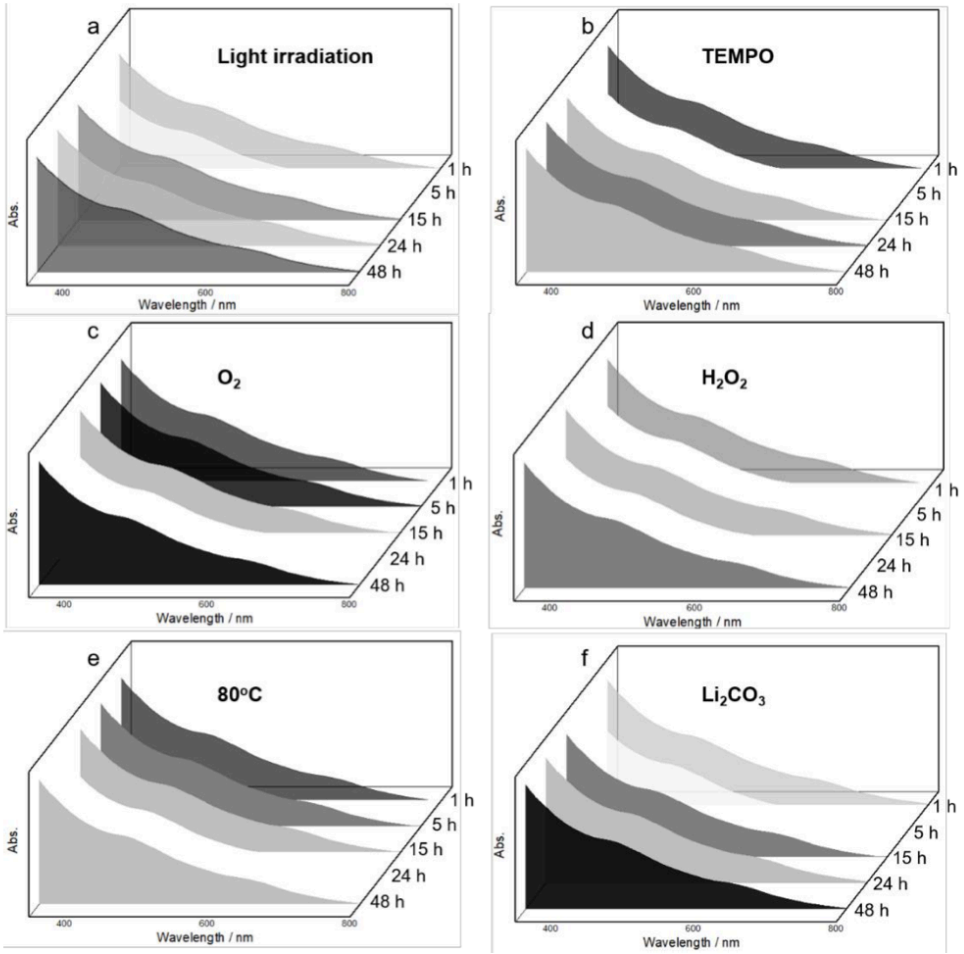

Supplementary Figure S4. Stability test of Au_8Cu_6 nanocluster. Time-dependent UV-vis spectra of Au_8Cu_6 dissolved in toluene with blue LED irradiation (a), single-electron oxidant TEMPO (b), two-electron oxidants O_2 (c) and H_2O_2 (d), high temperature (e), and basic conditions (f).

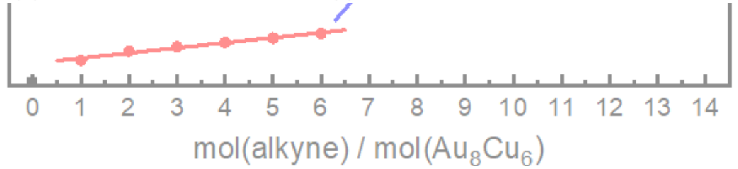

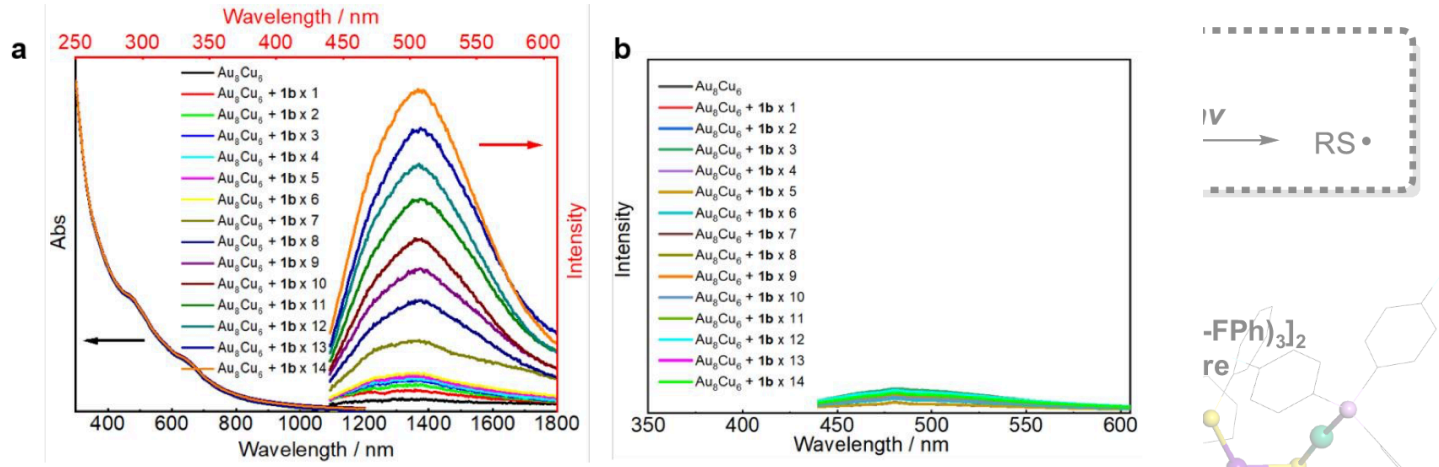

Supplementary Figure S5. Activation site test. (a) Absorption (left, black scale) and emission (right, red scale) spectra (λ_{ex} = 420 nm) of Au_8Cu_6 (solvent = DCM) with the addition of **1b** (4-fluorophenylacetylene) in the presence of lithium carbonate. (b) Emission spectra (λ_{ex} = 420 nm) of Au_8Cu_6 (solvent = DCM) with the addition of **1b** (4-fluorophenylacetylene) in the absence of lithium carbonate.

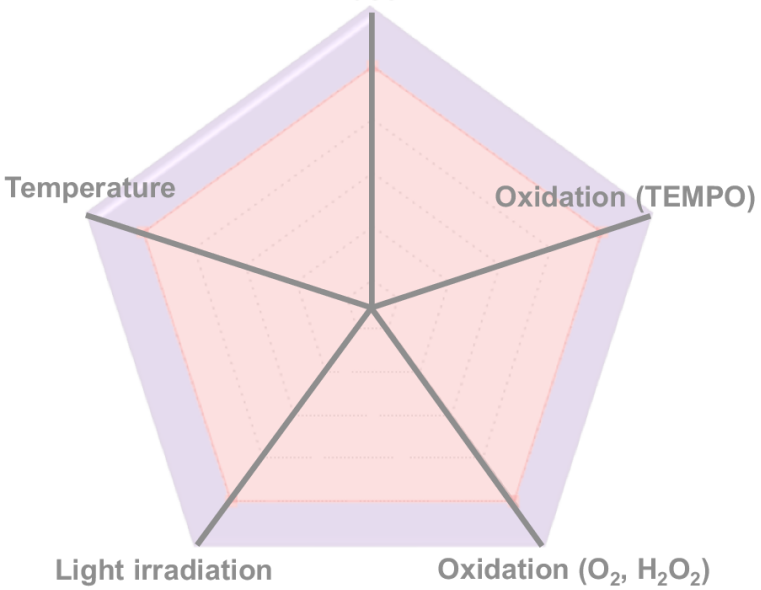

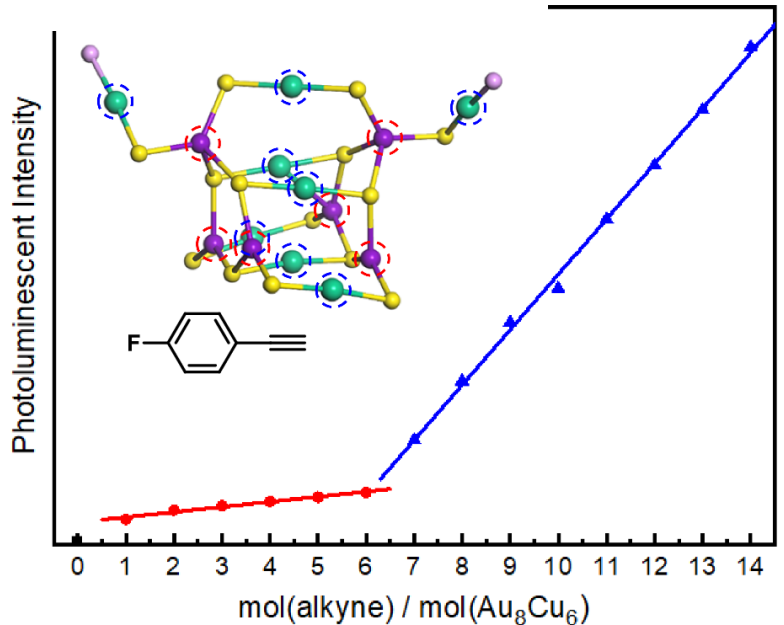

Optimization of reaction conditions

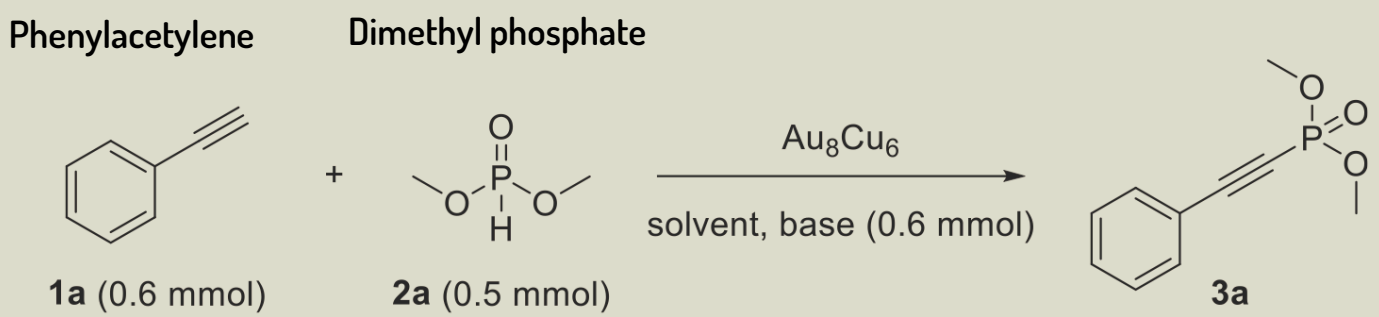

Entry	Irradiation	Solvent	Base	Catalyst amount, (mol%)	Time, (h)	Yield of 3a, (%)
1	Blue LED	THF	K_2CO_3	0.04	8	0
2	Blue LED	THF	K_2CO_3	0.04	8	41
3	Blue LED	MeOH	K_2CO_3	0.04	8	68
4	Blue LED	toluene	K_2CO_3	0.04	8	30
5	Blue LED	MeCN	K_2CO_3	0.04	8	Trace
6	Blue LED	MeOH	Na_2CO_3	0.04	8	14
7	Blue LED	MeOH	Cs_2CO_3	0.04	8	51
8	Blue LED	MeOH	Li_2CO_3	0.04	8	85
9	Blue LED	MeOH	Et_3N	0.04	8	67
10	Yellow LED	MeOH	Li_2CO_3	0.04	8	Trace
11	Green LED	MeOH	Li_2CO_3	0.04	8	Trace
12	Blue LED	MeOH	Li_2CO_3	0.04	4	87
13	Blue LED	MeOH	Li_2CO_3	0.005	4	85

Blue LED: 456 nm

Supplementary Table S1. Catalytic activity of different catalysts in mono-functionalization of alkynes.

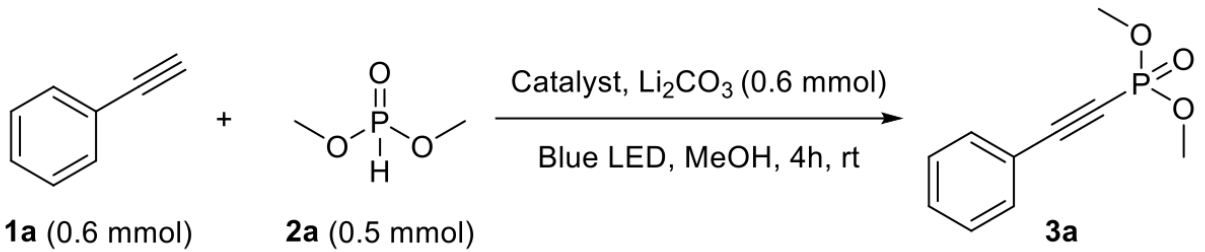

1a (0.6 mmol) **2a** (0.5 mmol) **3a**

Entry	Catalyst (loading, mol%)	Yield (%)
1	CuCl (0.5)	35
2	CuCl (0.005)	trace
3	$Au_{25}(SR)_{18}$ (0.5)	trace
4	$Au_{25}(SR)_{18}$ (0.005)	trace
5	$Au_8(PNP)_4$ (0.5)	trace
6	$Au_8(PNP)_4$ (0.005)	trace
7	$Cu_{25}H_{22}[P(4\text{-}FPh)_3]_{12}$ (0.5)	64
8	$Cu_{25}H_{22}[P(4\text{-}FPh)_3]_{12}$ (0.005)	trace
9	$Au_2Cu_6(PPh_2Py)_2(SC_{10}H_{15})_6$ (0.5)	42
10	$Au_2Cu_6(PPh_2Py)_2(SC_{10}H_{15})_6$ (0.005)	trace
11	$Au_8Cu_6(SPh)_{14}[P(4\text{-}FPh)_3]_2$ (0.5)	89
12	$Au_8Cu_6(SPh)_{14}[P(4\text{-}FPh)_3]_2$ (0.005)	85

3

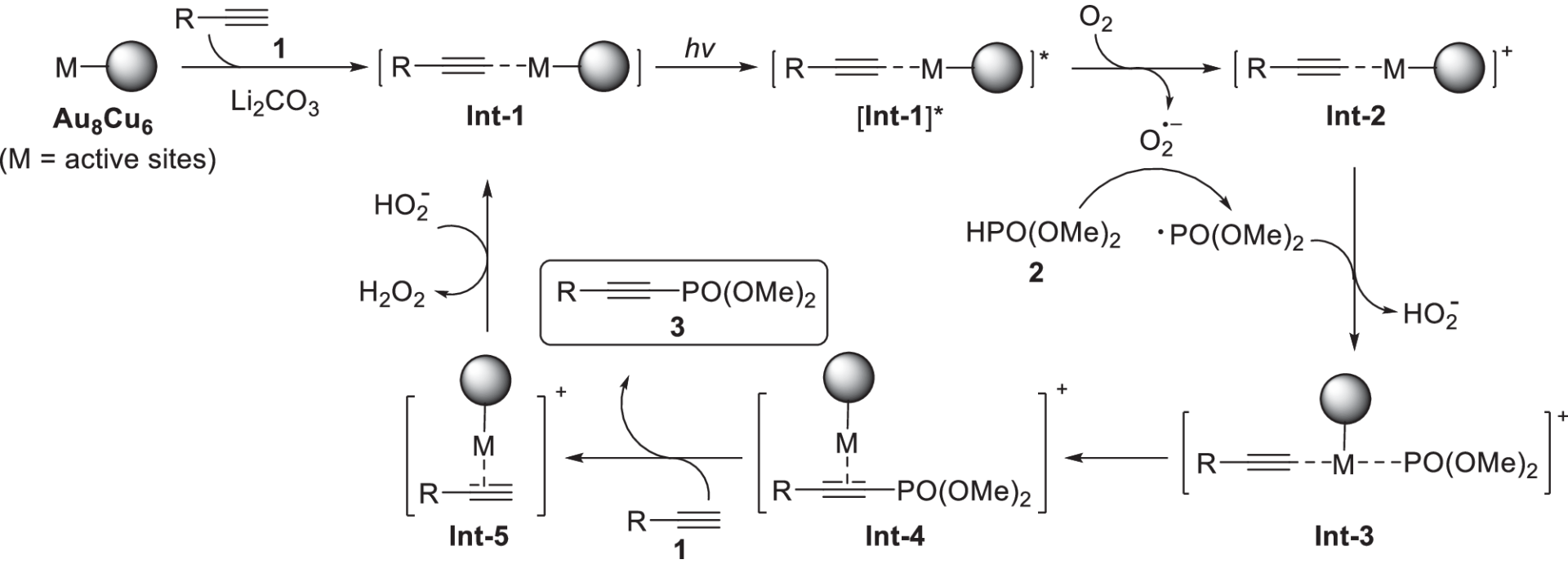

The sphere represents the main body of Au_8Cu_6 nanocluster, and M represents the activation site on the surface of the nanocluster.

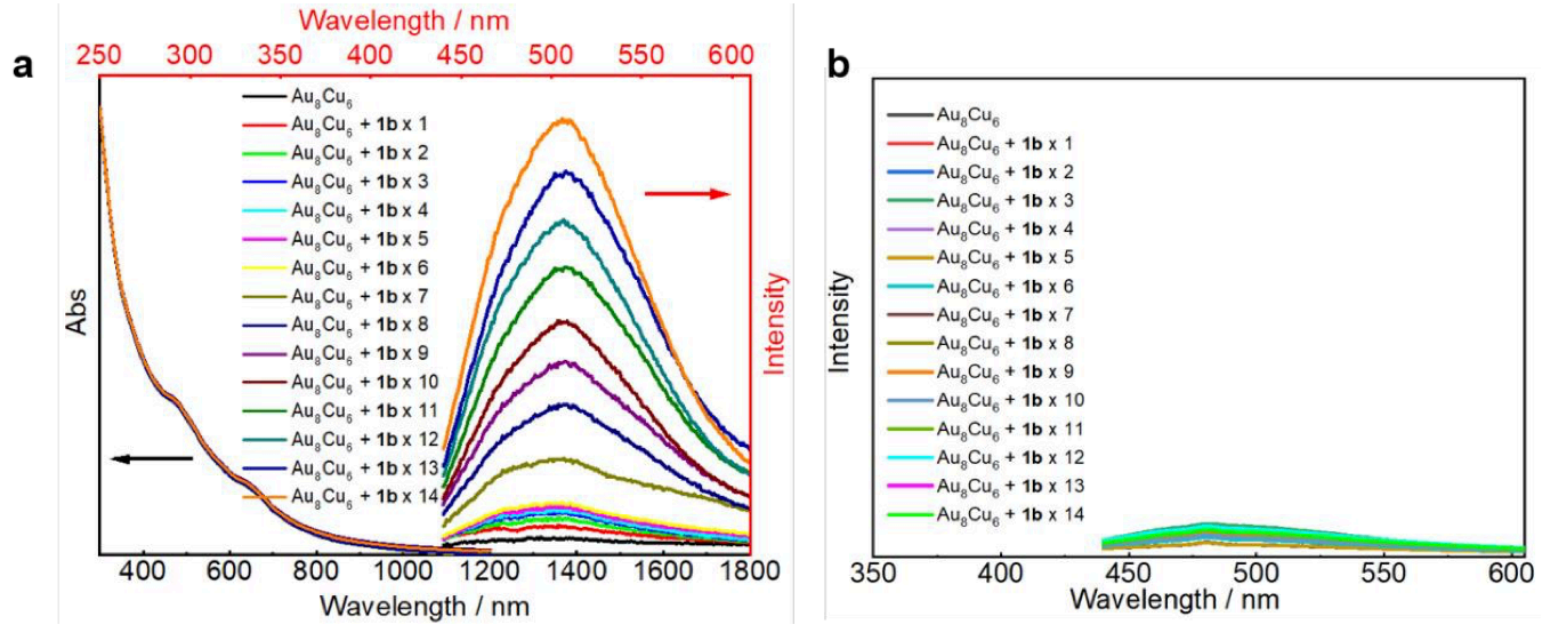

Supplementary Figure S5. Activation site test. (a) Absorption (left, black scale) and emission (right, red scale) spectra (λ_{ex} = 420 nm) of Au_8Cu_6 (solvent = DCM) with the addition of **1b** (4-fluorophenylacetylene) in the presence of lithium carbonate. (b) Emission spectra (λ_{ex} = 420 nm) of Au_8Cu_6 (solvent = DCM) with the addition of **1b** (4-fluorophenylacetylene) in the absence of lithium carbonate.

3

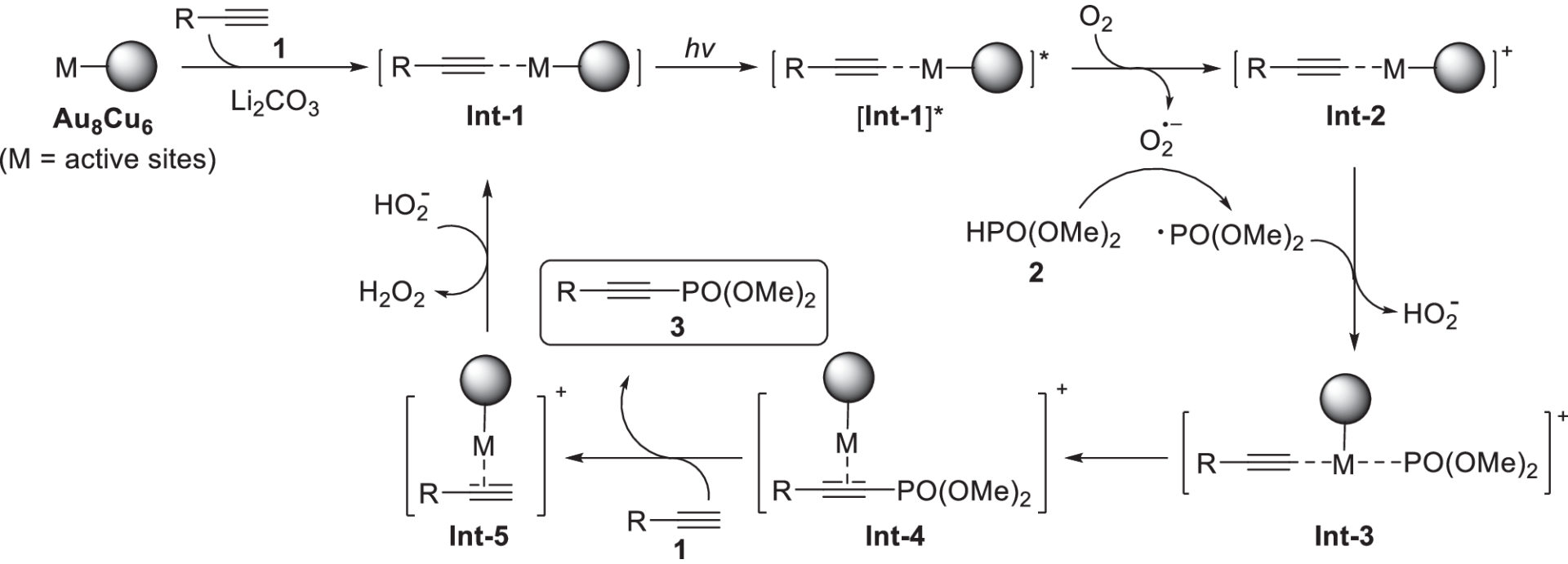

The sphere represents the main body of Au_8Cu_6 nanocluster, and M represents the activation site on the surface of the nanocluster.

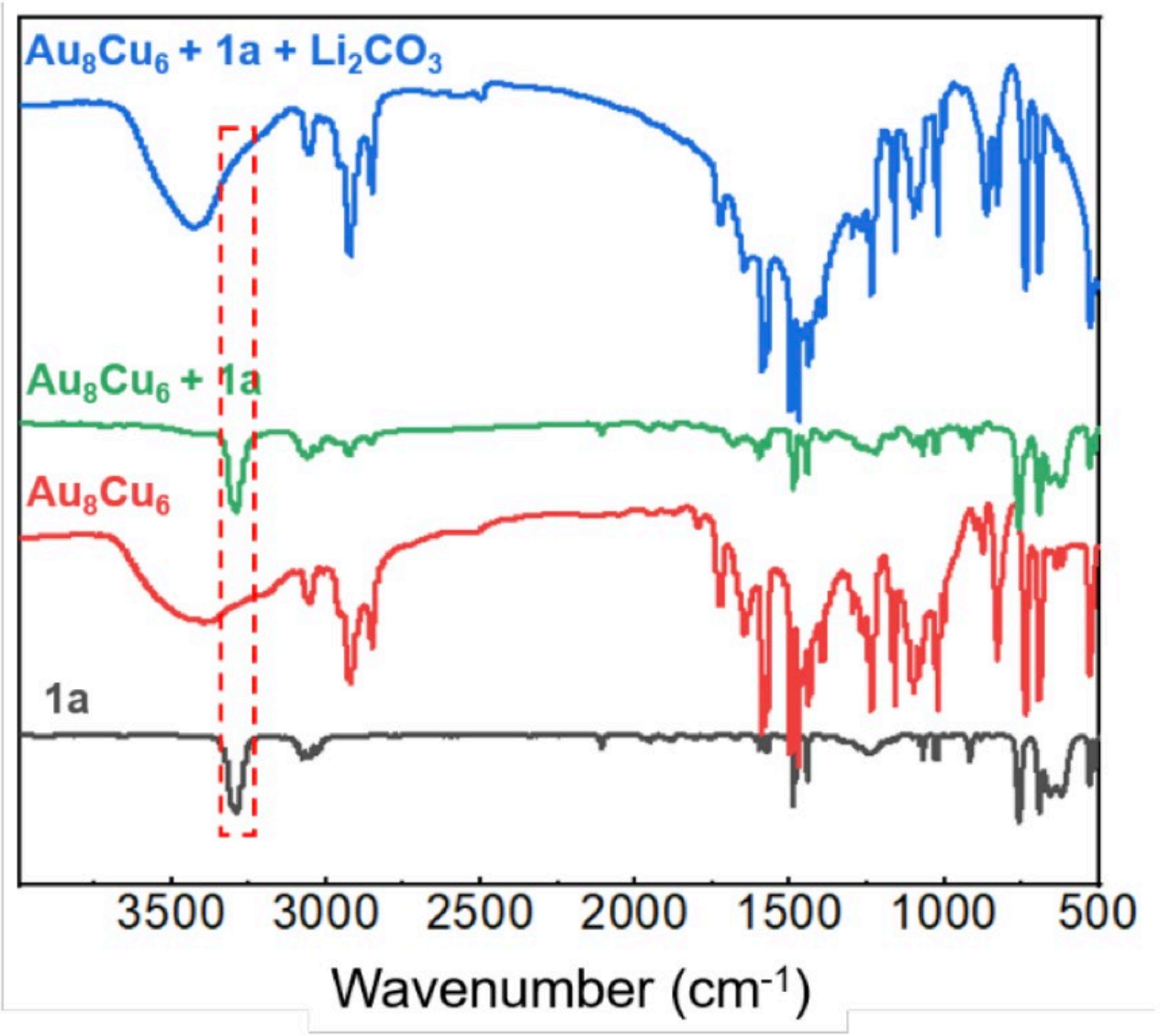

For infrared spectra, the comparison of the spectra of Au_8Cu_6, alkyne 1a, [Au_8Cu_6 + 1a] and [Au_8Cu_6 + 1a + Li_2CO_3] demonstrate that vibration of C(sp)–H of alkyne 1a at 3300 cm^{-1} disappeared in [Au_8Cu_6 + 1a + Li_2CO_3], while this vibration absorption peak is still visible in [Au_8Cu_6 + 1a].

3

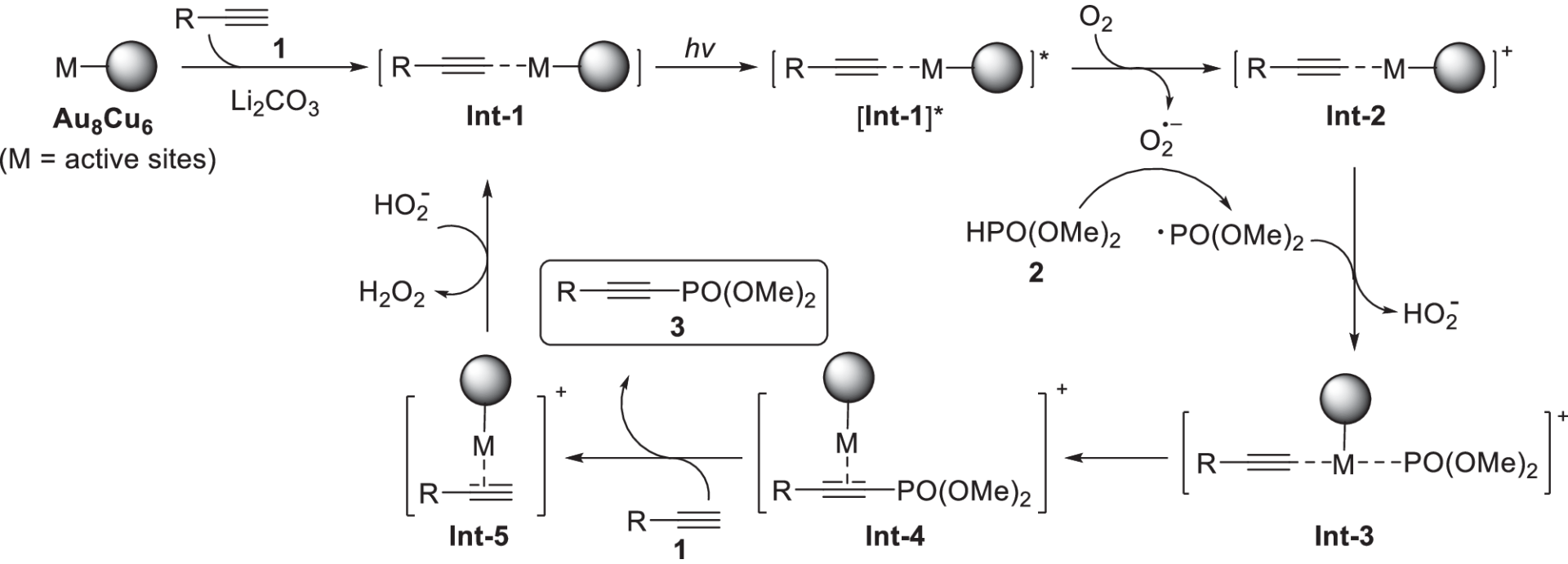

The sphere represents the main body of Au_8Cu_6 nanocluster, and M represents the activation site on the surface of the nanocluster.

2

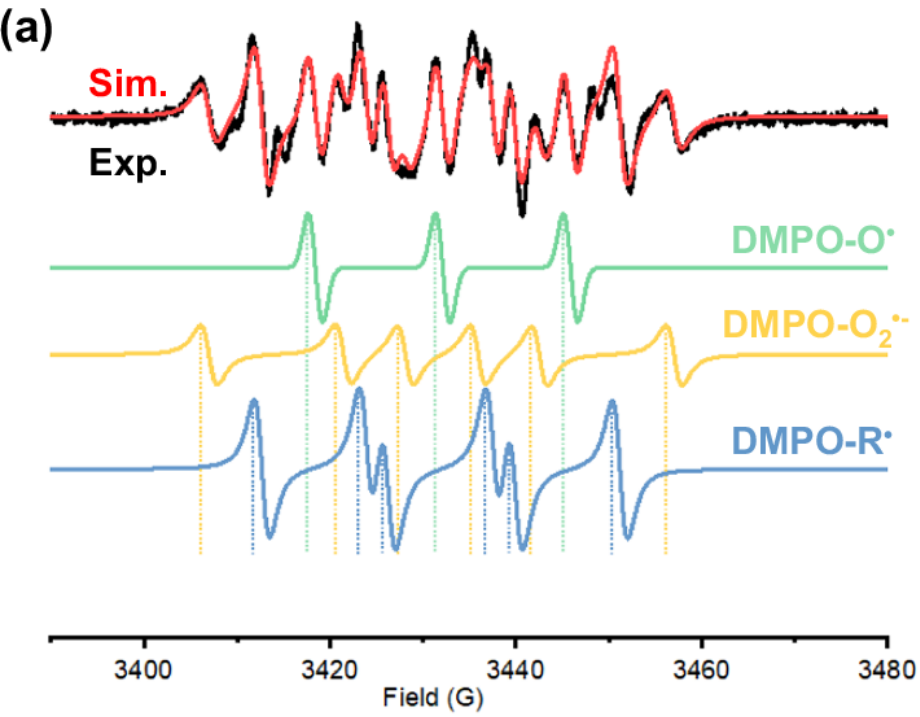

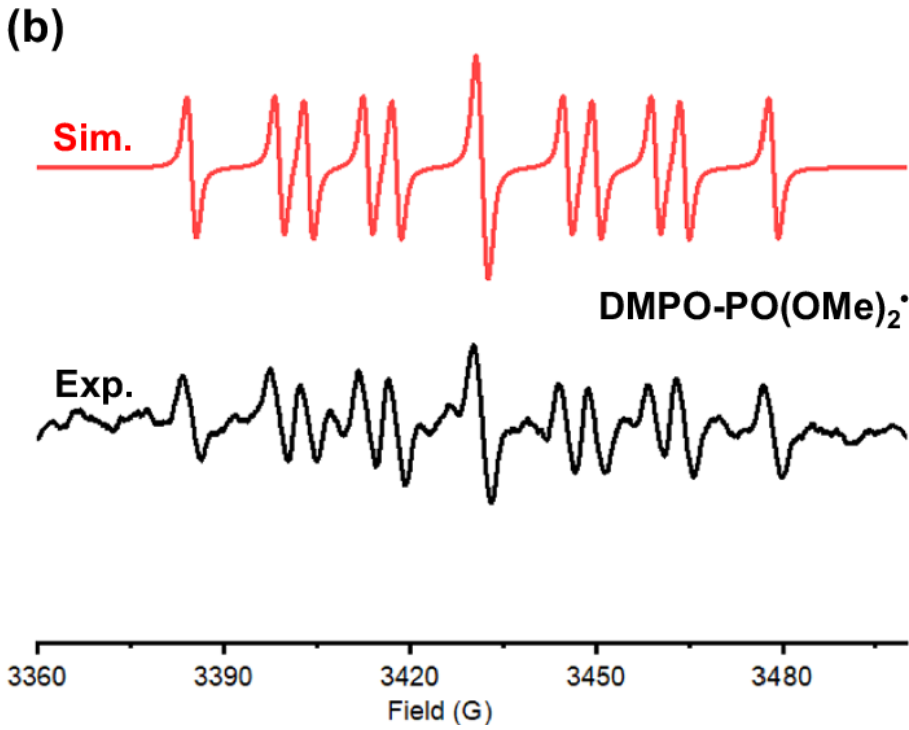

a The experimental (black) EPR spectrum of [Au_8Cu_6 + Li_2CO_3 + 1a] in the presence of O_2 and light irradiation with DMPO as the radical scavenger. The simulated (red) EPR spectrum is composed of the signals of DMPO-O• (green curve), DMPO-$O_2^{\bullet-}$ (yellow curve), and DMPO-R• (blue curve). b The experimental (black) EPR spectrum of [Au_8Cu_6 + Li_2CO_3 + 1a + 2a] in the presence of O_2 and light irradiation with DMPO as the radical scavenger. The simulated (red) EPR spectrum represents the DMPO-$PO(OMe)_2$•.

3

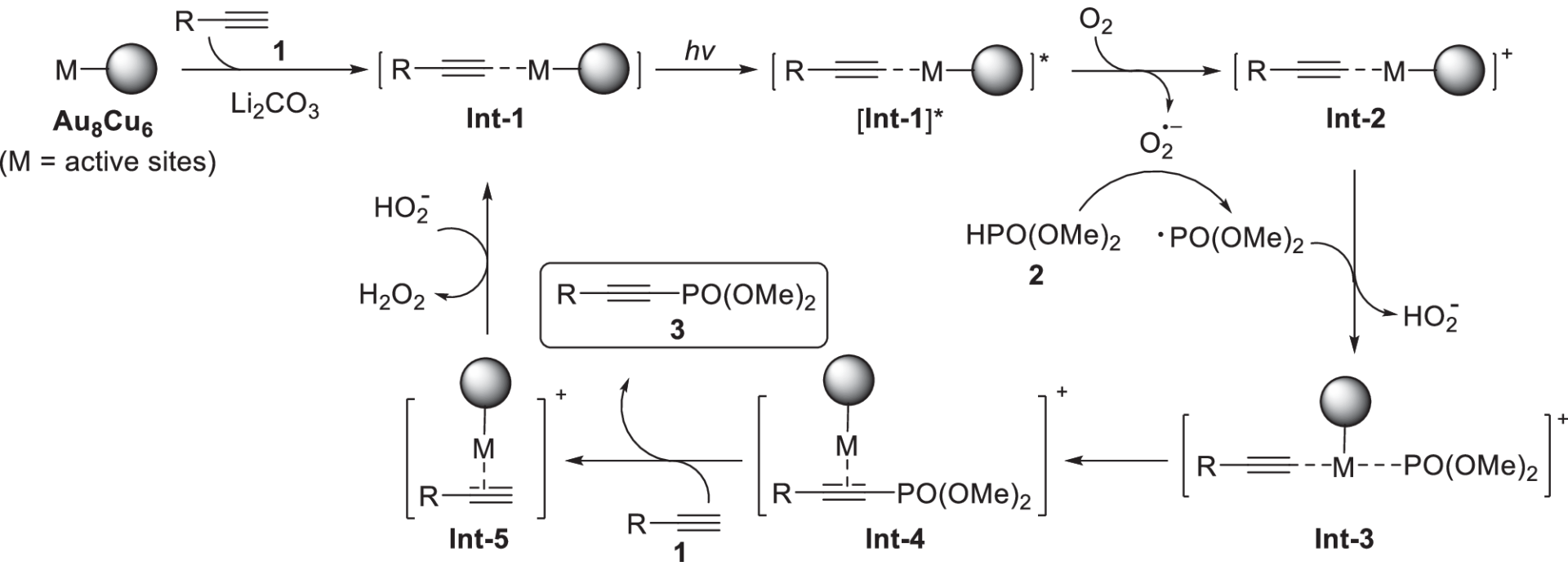

The sphere represents the main body of Au_8Cu_6 nanocluster, and M represents the activation site on the surface of the nanocluster.

4

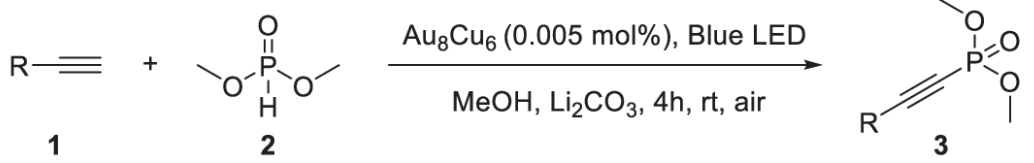

1 2 3

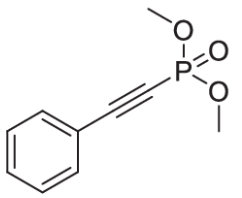

3a, 85%
TON = 17000

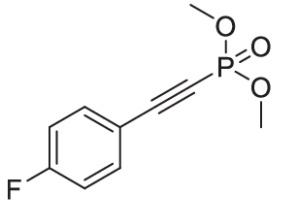

3b, 67%
TON = 13400

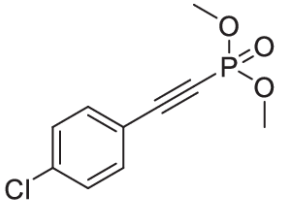

3c, 72%
TON = 14400

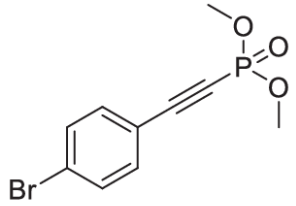

3d, 83%
TON = 16600

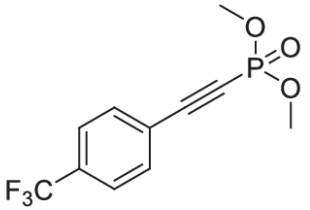

3e, 36%
TON = 7200

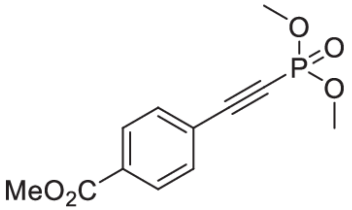

3f, 40%[a]
TON = 8000

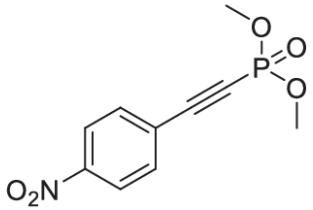

3g, 47%[a]
TON = 9400

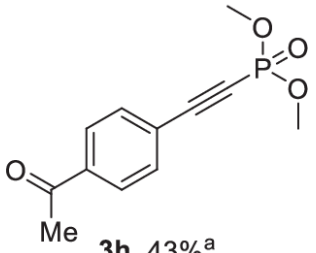

3h, 43%[a]
TON = 8600

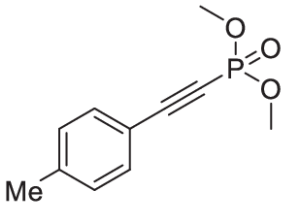

3i, 82%
TON = 16400

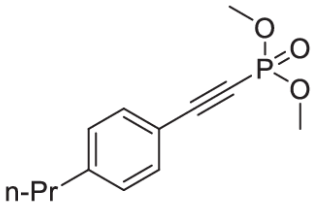

3j, 64%
TON = 12800

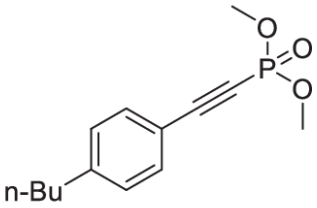

3k, 73%
TON = 14600

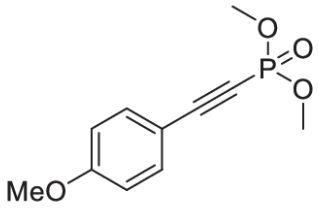

3l, 80%
TON = 16000

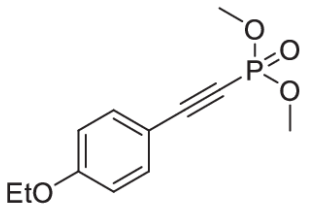

3m, 83%
TON = 16600

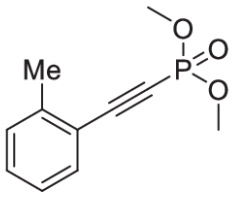

3n, 86%
TON = 17200

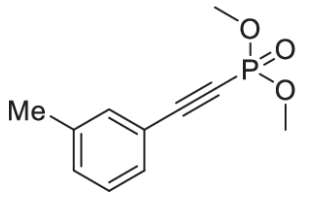

3o, 79%
TON = 15800

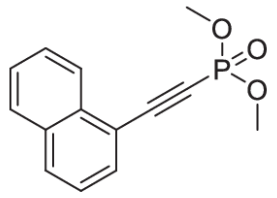

3p, 32%
TON = 6400

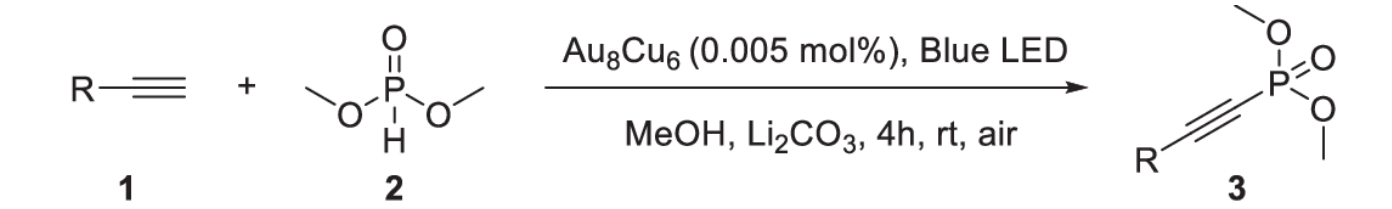

1 **2** **3**

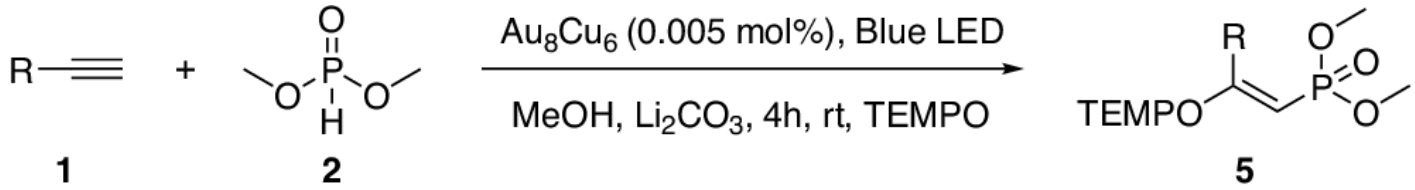

1 **2** **5**

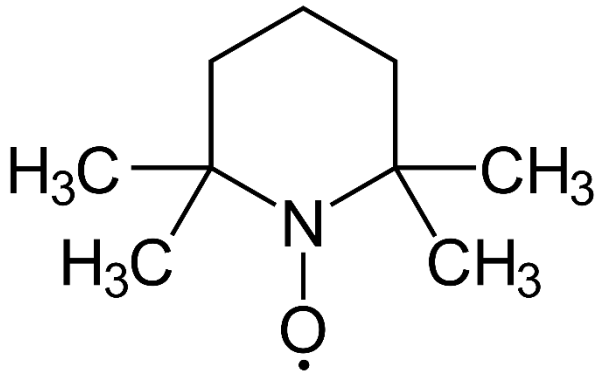

(2,2,6,6-Tetramethylpiperidin-1-yl)oxyl

TEMPO

5

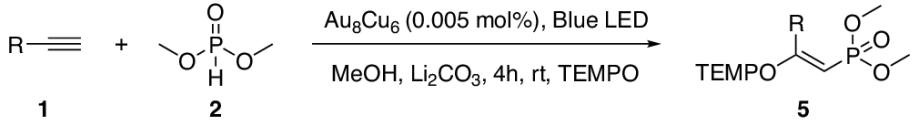

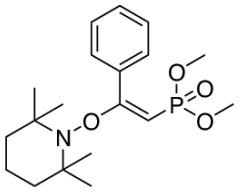

5a, 92%
TON = 18400

	Au_8Cu_6	**5a**
Gram-scale synthesis	0.6 mg	1.06 g
Catalyst recycling	fresh	92%
	recovered	92%

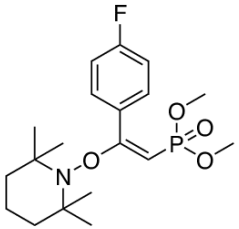

5b, 90%
TON = 18000

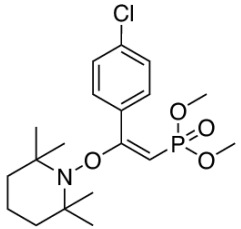

5c, 91%
TON = 18200

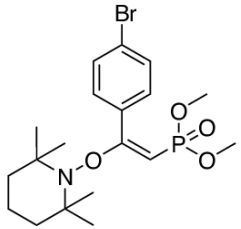

5d, 91%
TON = 18200

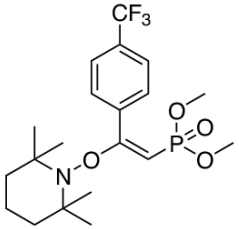

5e, 78%
TON = 15600

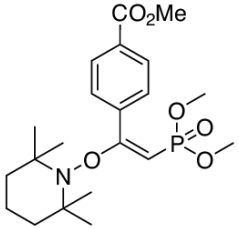

5f, 42%
TON = 8400

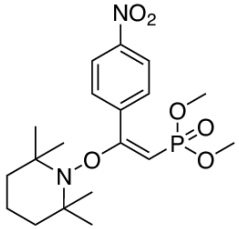

5g, 76%
TON = 15200

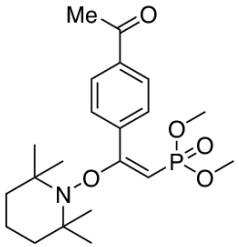

5h, 55%[a]
TON = 11000

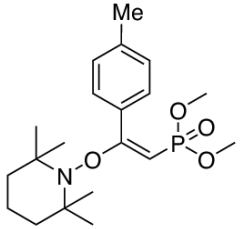

5i, 88%
TON = 17600

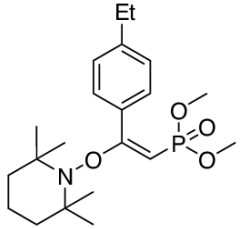

5j, 90%
TON = 18000

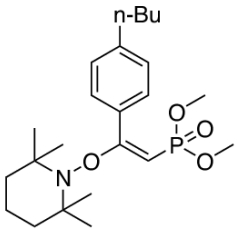

5k, 88%
TON = 17600

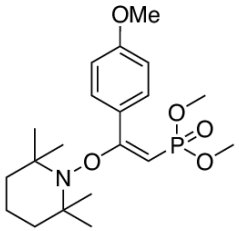

5l, 87%
TON = 17400

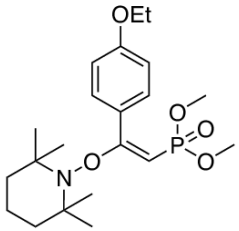

5m, 88%
TON = 17600

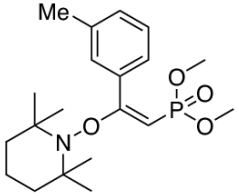

5n, 89%
TON = 17800

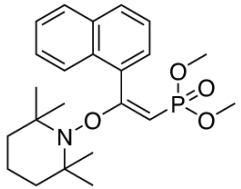

5o, 47%
TON = 9400

≡

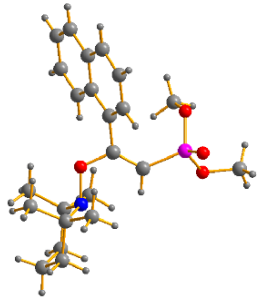

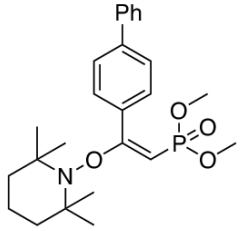

5p, 69%
TON = 13800

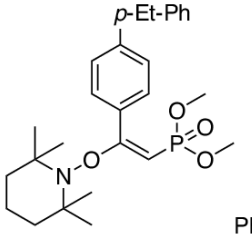

5q, 69%
TON = 13800

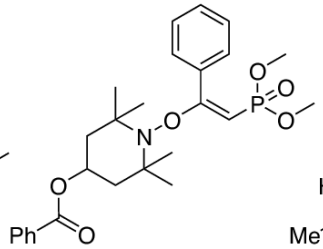

5r, 53%
TON = 10600

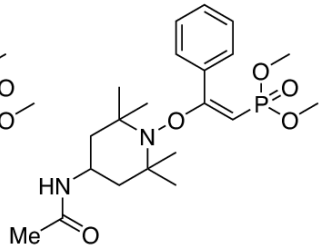

5s, 51%[a]
TON = 10200

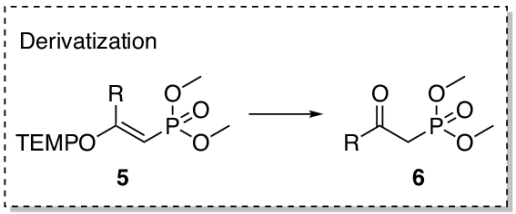

6

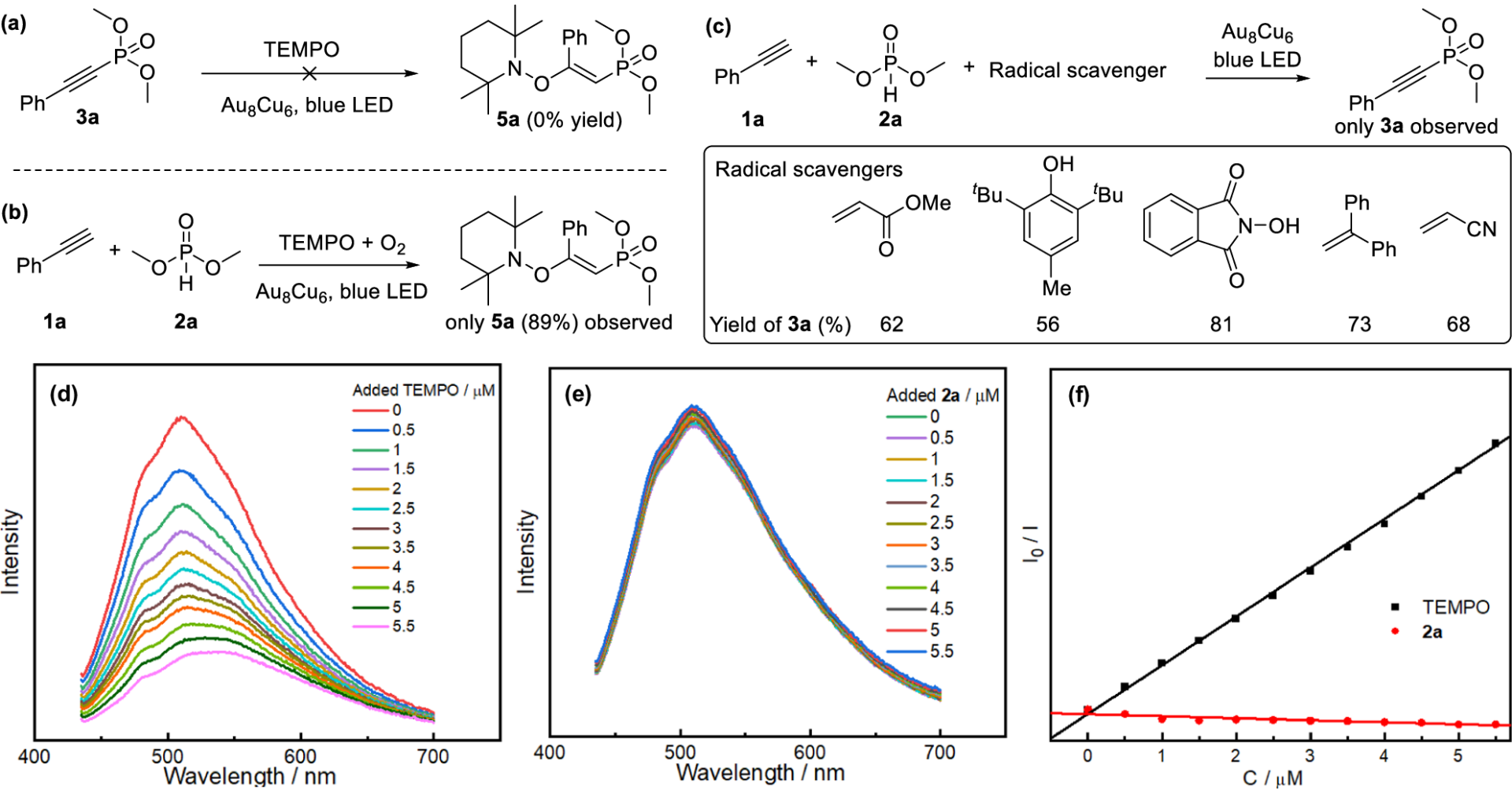

a–c Control experiments. d–f Photoluminescent quenching experiments of [Au_8Cu_6 + Li_2CO_3 + alkyne 1a] with TEMPO (d, f) or H-phosphonate 2a (e, f). Colors in d, e represent the photoluminescent spectra of [Au_8Cu_6 + Li_2CO_3 + alkyne 1a] under different concentrations of additives (solvent = DCM). Black and red curves in f represent the intensity changes of photoluminescent spectra in (d, e).

7

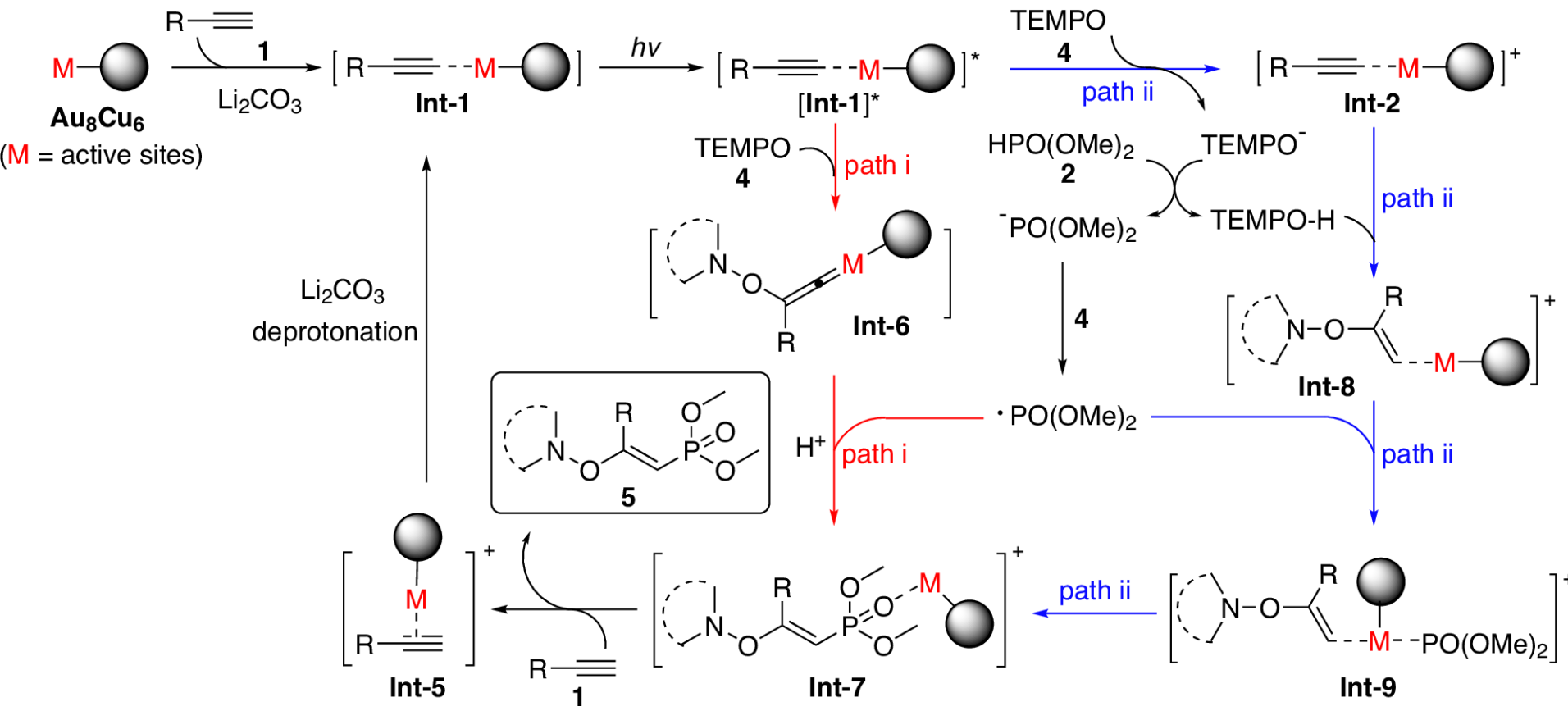

The sphere represents the main body of the Au_8Cu_6 nanocluster, and M represents the activation site on the surface of the nanocluster. Blue and red curves represent the two possible pathways of the catalytic reaction.

Summary

- Following the photochemical reduction–oxidation cascade method, they synthesized an Au_8Cu_6 nanocluster that features high durability toward light irradiation and formally full +1 charged metal atoms on the surface.
- This nanocluster demonstrates high catalytic activity, switchable selectivity, and catalyst recyclability, enabling efficient oxidative functionalization of alkynes.
- Mono-functionalized alkynylphosphonates and di-functionalized alkenylphosphonates were selectively obtained in the presence of O_2 and TEMPO as the oxidant, respectively.
- In-depth mechanism studies revealed the origin of the selectivity.